Pb_m−Phenyl ($m = 1-5$) Complexes: an Anion Photoelectron Spectroscopy and Density Functional Study

Hongtao Liu, Xiaopeng Xing, Shutao Sun, and Zhen Gao

Beijing National Laboratory for Molecular Sciences (BNLMS), State Key Laboratory of Molecular Reaction Dynamics, Center of Molecular Science, Institute of Chemistry, Chinese Academy of Sciences, Beijing 100080, P. R. China

Zichao Tang*

State Key Laboratory of Molecular Reaction Dynamics, Dalian Institute of Chemical Physics, Chinese Academy of Sciences, Dalian 116023, P.R. China

Received: March 21, 2006; In Final Form: May 11, 2006

The phenyl−lead metal complexes ($[Pb_mC_6H_5]^-$) produced from the reactions between benzene and lead clusters formed by laser ablation on a lead solid sample are studied by photoelectron spectroscopy (PES) and density functional theory (DFT). The adiabatic electron affinities (EAs) of $[Pb_mC_6H_5]^-$ are obtained from PES at 308 nm, and the differences between the PES of $[Pb_mC_6H_5]^-$ and the PES of Pb_m^- are discussed in detail. The results reveal that the phenyl group binds perpendicularly on lead clusters through the Pb−C σ bond and the complexes have a closed shell structure. Calculations with DFT are carried out on the structural and electronic properties of $[Pb_mC_6H_5]^-$, and the adiabatic detachment energy for the optimized structures of anion are in agreement with the experimental PES results. The density of states (DOS) calculated is compared with experimental PES and is discussed. The most possible structures for each species are concluded, and the bonding between Pb and phenyl is analyzed, which also proves that the phenyl group binds perpendicularly on lead clusters through the Pb−C σ bond.

1. Introduction

The chemisorption and dissociation of benzene on the metal cluster surfaces and the structure of metal/benzene complexes have been studied extensively in theory and experiment.[1−22] For example, Kaya and co-workers[16−18] reported the sandwich structure (Sc, Ti, V) and rice-ball structures (Fe, Co, Ni) of metal/benzene complexes. Bowen and co-workers[9−11] using photoelectron spectroscopy (PES) studied the electronic structure of M/benzene (M = Ti, Co, Ni) cluster anions. Theoretical investigations to understand the structures and properties of these metal−benzene association complexes were recently conducted by Rao and co-workers.[19,20,23] While these studies focus mainly on the reaction of transition metal species with benzene molecules, work is still required on the reactions of main group metal clusters with benzene molecules.

Lead is the heaviest element in group IV. It is known that the bulk lead solid is metallic, in contrast to the semiconductors of silicon and germanium crystals. The structure of lead clusters is intriguing among the clusters of group IV elements due to its large relativistic effects and especially, spin−orbit coupling.[24,25] Thus it is particularly interesting to exploit whether the lead cluster is semimetallic or metallic. Negishi and coworks,[26] using PES and a halogen-doping method, studied the electronic properties of group IV cluster anions, and found that the properties of Pb_n clusters are different from those of the other group IV clusters, probably exhibiting a metallic nature. However, Wang and co-workers[27] studied the lowest energy structures and electronic properties of lead clusters by density-functional-theory (DFT) calculation, and they found that the structures of smaller Pb_n ($n \leq 10$) clusters are similar to those of Si and Ge clusters and the covalent-to-metallic transition starts from Pb_{11}. In addition to its structure and property investigations, the study on the reactivity of lead cluster ions is also of fundamental interest. As early as 1972, Castleman and co-workers[28] studied the gas-phase hydration of the monovalent lead ion using high-pressure mass spectrometry, and clusters of up to eight water molecules around a single lead ion were observed. Later the same group reported the clustering reaction of benzene with lead ions, and Pb^+−benzene displayed an unusually strong interaction.[29] In our publications,[30] the reactions of lead cluster anions with benzene were reported. The important intermediate series of products were [Pb_m−phenyl]$^-$ ($m = 1-5$), which were rare cases in chemistry.

The photoelectron spectroscopy (PES) is a well-known useful experimental technique for the investigations of molecular electronic and geometric structure of lead clusters.[26,31−33] Here we report the photoelectron spectroscopic study on anion [Pb_m−phenyl]$^-$ ($m = 1-5$), which were produced from reactions between benzene and vapor lead generated by laser ablation on a lead solid sample.[30] By combination of experimental and theoretical studies we have gained a significant understanding of bonding, geometric, and electronic structures of the [Pb_m−phenyl]$^-$ ($m = 1-5$). It is our hope that the reported results will aid in the deep study on physics and chemistry of lead cluster complexes.

2. Experimental Methods

The apparatus used in the experiments mainly consists of a homemade reflectron time-of-flight mass spectrometer (RTOFMS)

* Address correspondence to this author. Phone: +86-411-84379365. Fax: +86-411-84675584. E-mail: zctang@dicp.ac.cn.

10.1021/jp0617470 CCC: $33.50
Published on Web 06/23/2006

with high resolution and a photoelectron spectrometer with magnetic-bottle type analyzer. The details of the apparatus have been published elsewhere,[34,35] and only an outline is given below.

The lead disk targets (99.9%) in the source chamber of RTOFMS are rotated and ablated by a pulsed laser beam (532 nm Nd:YAG laser, 10 Hz, 10 mJ/pulse). The laser-induced plasma is carried by molecular beam generated by a pulsed valve at a backing pressure of about 400 kPa of argon (purity 99.99%), in which benzene is seeded. The volume ratio of benzene in the mixed gas is about 0.2%. The Pb_m−phenyl cluster anion products from the reactions of lead and benzene are entrained by the carrier gas and undergo low pressure (10^{-2} Pa) in the source chamber. After passing a skimmer, all products enter into the acceleration area in the spectroscopic chamber (10^{-4} Pa). The negatively charged clusters are accelerated in the direction perpendicular to the molecular beam and are reflected toward to the detector, microchannel plates (MPC). The resolution ($M/\Delta M$) of RTOFMS is better than 2000, so it is easy to resolve the number of hydrogen atoms in the products. The products can be mass selected by the timing probe. The anions are photodetached by a XeCl excimer laser (308 nm), and the photoelectrons detached are measured by the photoelectron spectrometry, a magnetic-bottle time-of-flight analyzer, calibrated by the known spectra of Ag^- and Au^-. The energy resolution of the photoelectrons is approximately 70 meV for 1 eV electrons.

3. Computational Methods

Full geometric optimization for all the cluster structures is performed with relativistic density functional calculations at the level of generalized gradient approach, using a Perdew−Wang exchange-correlation functional.[36] The zero-order regular approximation Hamiltonian is used to account for the scalar (mass velocity, Darwin, and spin−orbit) relativistic effects.[37] The standard Slater-type orbital basis sets of the triple-ζ plus two polarization functions (TZ2P) are used for the orbitals of Pb, C, and H atoms. And the frozen core ($1s^2-4f^{14}$) approximation is used for Pb. All the calculations are accomplished with the Amsterdam density functional (ADF 2002) programs. It was shown previously that these theoretical methods were suitable for study on the metal clusters.[38]

4. Results and Discussion

4.1. PES Study on $[Pb_m(C_6H_5)]^-$ Complexes. The photoelectron spectra (PES) of Pb_m^- ($m = 2-5$) and $[Pb_m(C_6H_5)]^-$ ($m = 1-5$) at 308 nm are shown in Figure 1. It is supposed that the anions are in their electronic ground state due to the cooling in supersonic expansion. Each of these photoelectron spectra represents a transition from the ground state of the anions to the ground or excited electronic states of the neutrals. Because the photodetachment process is much faster compared with the movement of the nuclei, PES provides the electronic and vibrational information of the neutral species with the anionic cluster geometry. EA is defined as the energy of the origin transition between the ground state of the anion and the ground state of the neutral. As can be seen in Figure 1, every position, indicated with the arrow, is evaluated to be the EA of the corresponding complexes. The evaluation has considered the instrumental resolution (70 meV/1 eV). The broad features at the lower binding energy side of the spectra of $[Pb_m(C_6H_5)]^-$ ($m = 3-5$) are caused by the isomers or are due to small contamination. The EA values are listed in the Table 1. The measured EA values of Pb_m^- ($m = 2-5$) and their spectra

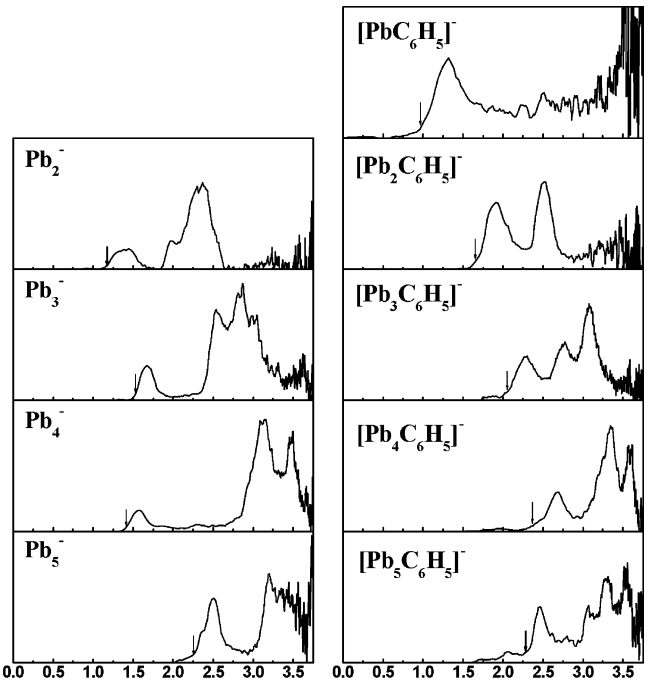

Figure 1. Photoelectron spectra of Pb_m^- ($m = 2-5$) and $[Pb_mC_6H_5]^-$ ($m = 1-5$) at 308 nm (4.03 eV) photon.

TABLE 1: Observed Electron Affinity for Pb_m and $Pb_m(C_6H_5)$ ($m = 1-5$) (Uncertainty within ±35 meV)

m	Pb_m^- EA (eV)	$[Pb_mC_6H_5]^-$ EA (eV)
1	(0.365[a])	1.01
2	1.21 (1.37,[b] 1.45[c])	1.70
3	1.54 (1.70[c])	2.03
4	1.40 (1.55,[c] 1.37[d])	2.35
5	2.26 (2.35,[c] 2.17[d])	2.29

[a] Reference 39: $(6p^2)\ ^3P_0 \leftarrow (6p^3)\ ^4S_{3/2}$. [b] Reference 33: according to the Franck−Condon simulation. [c] Reference 31: the maximum of the first feature. [d] Reference 26: threshold of the electron detachment.

features are consistent with the results in refs 26, 31, 33, and 39 within experimental error.

In comparison of the electron detachment threshold, EA, of every $[Pb_m(C_6H_5)]^-$ ($m = 1-4$) is comparatively higher than that of the corresponding naked lead clusters Pb_m^-. This can be understood with molecular orbital theory as follows. After the bonding of Pb_m^- with the phenyl group, the symmetries of the products are lowered and the original degenerate orbitals (for example, $6p_x6p_y6p_z$ for Pb^-, $6p\pi$ for Pb_2^-, etc.) are transformed into nondegenerated ones. The MOs near the HOMO are rearranged and have a lower energy level with the contribution of the forming Pb−C bond. Therefore the closed shell structures of the electron for ground state $[Pb_m(C_6H_5)]^-$ are expected to have a total even number of electrons. The facts as above could cause the enhancement of the electron detachment threshold. However, the $[Pb_5C_6H_5]$ complex is an exception. Its EA is 2.29 eV, close to the EA value of Pb_5, and the photoelectron spectra of $[Pb_5C_6H_5]^-$ and Pb_5^- have a similar energy gap (between the first feature and the second feature) of about 0.7 eV. Furthermore, Pb_5 has an especially higher EA value than its neighbors ($m = 2-4$). The explanation is that Pb_5^-, like Pb_5, has a structure close to the Zintle configuration (trigonal bipyramid) of Pb_5^{2-},[24,40] with a difference of just the electron number. After absorbing phenyl, the original trigonal

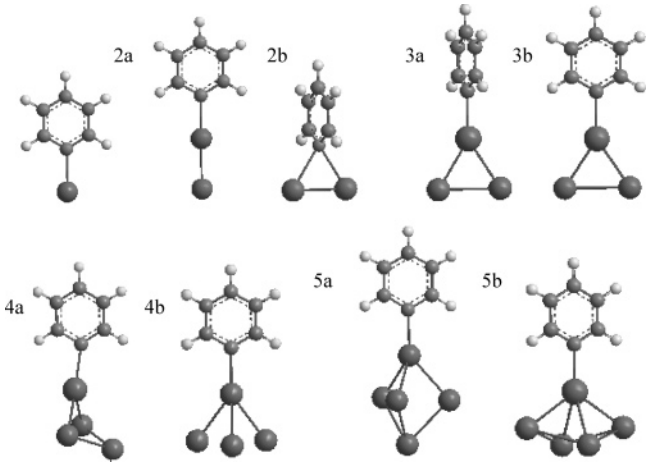

Figure 2. Optimized structures for neutral and anionic complexes of $Pb_mC_6H_5$ ($m = 1-5$). See Table 2 for structural parameters.

bipyramid structure of Pb_5 does not change much and the orbital distribution of the electrons of the Pb_5 is not much influenced. Therefore, the EA value and the feature of the spectrum of $Pb_5C_6H_5$ are close to the case of Pb_5. Further description of this result with the help of theoretic calculation can be seen in Part 4.

For $[Pb_m(C_6H_5)]^-$ ($m = 4, 5$), the PES (including the EAs, the slow rising tails, and the first and the second electron peaks) are very similar to that of $[Pb_mF]^-$ ($m = 4, 5$), in which the F atom surely combines with Pb_m with a single chemical bond.[26] This is evidence that the phenyl group absorbs on the surface of the lead cluster through a single Pb−C chemical bond. In conclusion of PES obtained from experiments, it can be suggested that $[Pb_m(C_6H_5)]^-$ species have the Pb−C bond and closed shell electronic configuration. These characteristics are also confirmed by the DFT calculations on $[Pb_m(C_6H_5)]^-$, shown below.

4.2. Theoretical Calculated Low-Energy Structures. For both the neutral $Pb_mC_6H_5$ and anion $[Pb_mC_6H_5]^-$ ($m = 1-5$), we considered a variety of structures. The optimized low-energy structures are shown in Figure 2, and their structural and energetic characteristics are summarized in Table 2. For neutral PbC_6H_5 and the anion $[PbC_6H_5]^-$, their optimized structures are C_{2v} symmetry, in which the phenyl group couples with the lead atom through the Pb−C bond and the phenyl and lead atoms are coplanar. The other initial structures collapse to this geometry during optimization. For neutral $Pb_2C_6H_5$ and the anion $[Pb_2C_6H_5]^-$, there are two low-energy isomeric structures (**2a**, **2b**) which all have C_{2v} symmetry. Isomer **2a** is that where the phenyl group couples with the lead atom through the Pb−C bond and the phenyl and lead atoms are coplanar. Isomer **2b** is that where the Pb−Pb bond is perpendicular to the plane of the phenyl group. For neutral $Pb_3C_6H_5$ and the anion $[Pb_3C_6H_5]^-$, also the two low-energy conformational isomers (**3a**, **3b**) exist. Isomer **3a** is that where the phenyl group is perpendicular to the Pb_3 plane, and isomer **3b** is that where the phenyl group rotates to be in the Pb_3 plane. The two structures have C_{2v} symmetry. For neutral $Pb_4C_6H_5$ and the anion $[Pb_4C_6H_5]^-$, the two structures **4a** and **4b** shown in Figure 2 have C_s symmetry. Isomer **4a** has the lowest energy, in which the Pb_4 group has a butterfly structure and couples with the phenyl group through the Pb−C bond. Isomer **4b** has an energy a little bit more than that of **4a**, in which the Pb_4 group has a tetrahedron structure and couples on the phenyl group through the Pb−C bond. For neutral $Pb_5C_6H_5$ and the anion $[Pb_5C_6H_5]^-$, the two optimized low-energy structures (**5a**, **5b**) are obtained, in which the two

TABLE 2: Various Structural and Energetic Characteristics for Neutral and Anionic Complexes of $Pb_mC_6H_5$ ($m = 1-5$)

						EA (eV)	
clusters	isomer	state	point group	R_{Pb-C} (Å)	ΔE^a (eV)	cal	exp[b]
PbC_6H_5		$^2B_2$	C_{2v}	2.30	0.00	0.94	1.01
$[PbC_6H_5]^-$		$^1A_1$	C_{2v}	2.32	0.00		
$Pb_2C_6H_5$	**2a**	$^2B_1$	C_{2v}	2.26	0.46	1.60	1.70
	2b	$^2B_2$	C_{2v}	2.54	0.00	1.51	
$[Pb_2C_6H_5]^-$	**2a**	$^1A_1$		2.30	0.37		
	2b	$^1A_1$		2.61	0.00		
$Pb_3C_6H_5$	**3a**	$^2B_1$	C_{2v}	2.24	0.02	1.93	2.03
	3b	$^2A_1$	C_{2v}	2.25	0.00	1.93	
$[Pb_3C_6H_5]^-$	**3a**	$^1A_1$	C_{2v}	2.31	0.02		
	3b	$^1A_1$	C_{2v}	2.34	0.00		
$Pb_4C_6H_5$	**4a**	$^2A''$	C_s	2.29	0.00	2.13	2.35
	4b	$^2A''$	C_s	2.29	0.17	1.51	
$[Pb_4C_6H_5]^-$	**4a**	$^1A'$	C_s	2.35	0.00		
	4b	$^1A'$	C_s	2.31	0.79		
$Pb_5C_6H_5$	**5a**	$^2A''$	C_s	2.25	0.00	2.51	2.29
	5b	$^2B_2$	C_{2v}	2.25	0.18	2.45	
$[Pb_5C_6H_5]^-$	**5a**	$^1A'$	C_s	2.29	0.00		
	5b	$^1A_1$	C_{2v}	2.29	0.24		

[a] ΔE is the difference of complex energy relative to the correspondingly lowest lying structure. [b] The uncertainty for the experimental EA is ±0.035 eV.

Pb_5 group structures are similar to that of the naked Pb_5 cluster, having a trigonal bipyramid structure. The difference between these two isomers is the Pb atom coupled by the phenyl group. In **5a** the phenyl group couples on the Pb_5 through one top lead atom, and in **5b** the phenyl group couples on the Pb_5 through one middle lead atom. So structure **5a** has C_s symmetry and structure **5b** has C_{2v} symmetry.

4.3. Assignments of the Complex Structures. In the following, we will confirm the structures of $Pb_mC_6H_5$ ($m = 1-5$) by calculating EAs using the relativistic DFT. The assignment of the most possible structures of $Pb_mC_6H_5$ is given on the basis of relative energies and comparisons between the theoretically calculated DOS and the experimental PES spectra. The structural assignment method has been widely used in cluster study.[27,38,41−45] EA is calculated as the difference between the total energies of the neutral and anion at their respective optimized structures. The theoretical DOS is shifted by setting the HOMO level of the spectra to give the negative of the DOS value for the complex. This is called the theoretically generalized Koopman theorem (GKT)[46]-shifted DOS.[43] The comparisons of theoretical results with experimental PES of $[Pb_mC_6H_5]^-$ are shown in Figures 3−7. Here it should be noticed that in comparison of

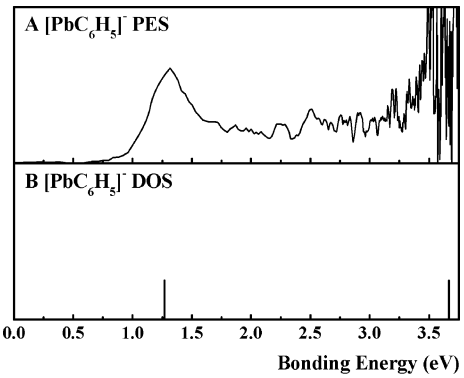

Figure 3. The comparison of PES of $[PbC_6H_5]^-$ with theoretical generalized Koopman theorem-shifted DOS for the optimized ground-state structure of $[PbC_6H_5]^-$.

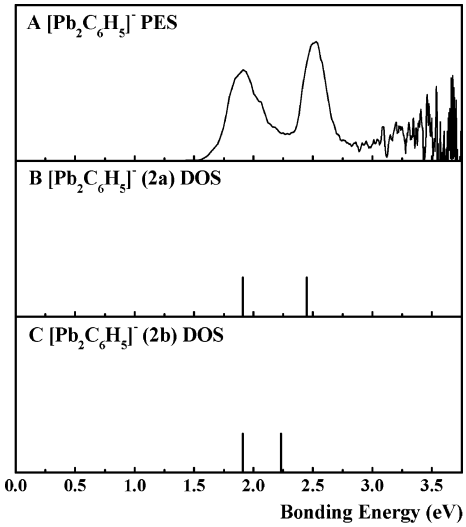

Figure 4. The comparison of PES of $[Pb_2C_6H_5]^-$ with theoretical generalized Koopman theorem-shifted DOS for structures **2a** and **2b** of $[Pb_2C_6H_5]^-$.

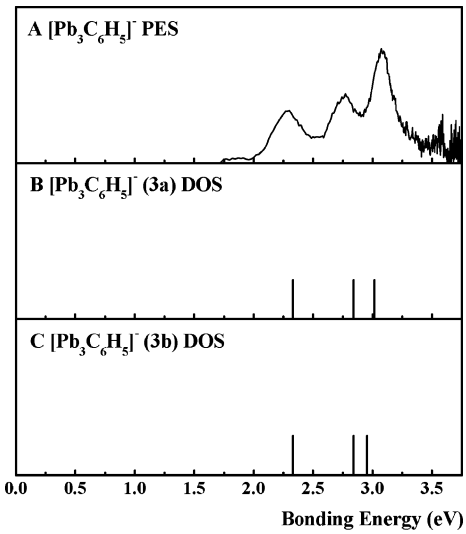

Figure 5. The comparison of PES of $[Pb_3C_6H_5]^-$ with theoretical generalized Koopman theorem-shifted DOS for structures **3a** and **3b** of $[Pb_3C_6H_5]^-$.

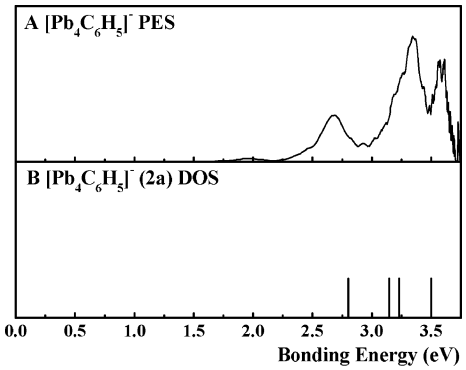

Figure 6. The comparison of PES of $[Pb_4C_6H_5]^-$ with theoretical generalized Koopman theorem-shifted DOS for structure **4a** of $[Pb_4C_6H_5]^-$.

the DOS spectra with the PES spectra, the importance is the electron binding energy corresponding to each feature and not the relative intensity. The relative intensity also depends on other factors such as the unknown orbital-dependent photodetachment cross-section. So here the DOS is plotted as the stick spectrum

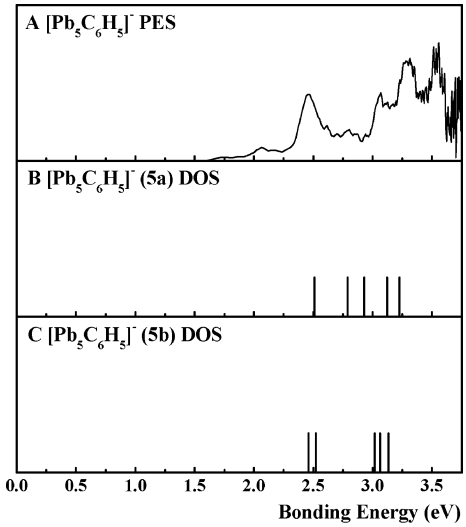

Figure 7. The comparison of PES of $[Pb_5C_6H_5]^-$ with theoretical generalized Koopman theorem-shifted DOS for structures **5a** and **5b** of $[Pb_5C_6H_5]^-$.

in Figure 3−7 by aligning the HOMO level of anions with the threshold peak, instead of the fitted DOS spectra.[43]

$[PbC_6H_5]^-$. The planar structure with C_{2v} symmetry, in which the phenyl group couples on the lead atom through the Pb−C bond, is clearly the ground state for both neutral and anionic complexes. The energy difference between the neutral and anionic structures (corresponding to the calculated EAs) is listed in Table 2. The calculated EA of PbC_6H_5 by the relativistic DFT is 0.94 eV. It is in good agreement with the experimental results of 1.01 eV. As shown in Figure 3, the energy gap between the HOMO levels in the DOS spectrum agrees reasonably well with the experimental PES spectrum. Thus it is suggested that only the ground state of anions contributes to the measured PES.

$[Pb_2C_6H_5]^-$. The energy separation between structures **2a** and **2b** is 0.46 eV for neutral and 0.37 eV for anions. Although structure **2b** has a lower energy than **2a**, the EA of structure **2a** is much closer and in good agreement with the experimental result of 1.70 eV (the EAs of structures **2a** and **2b** are 1.60 and 1.51 eV, respectively). Furthermore, the calculated DOS of structure **2a**, exhibiting a large HOMO−LUMO gap of the neutrals (Figure 4), is consistent with the measured PES. So it is likely that the planar structure (**2a**) of the phenyl group, coupling on the lead atom through a single Pb−C bond, is dominant in the anions $[Pb_2C_6H_5]^-$ produced in the experiments. By the above analysis, the structure of product $[Pb_2C_6H_5]^-$ is assigned to **2a** though **2a** is not the lowest energy structure. Of course, the total energy of the structures is a very important factor for the determination of the structures of the products, but it is not the only one.

$[Pb_3C_6H_5]^-$. The energies of these two structures (**3a**, **3b**) have almost the same value (the difference is 0.02 eV), and they also have the same calculated EA value of 1.93 eV, having good agreement with the experimental results of 2.03 eV. The two calculated DOS of structures **3a** and **3b** are compared with experimental PES as shown in Figure 5. It can be concluded that **3a** matches that of the experiment well and **3b** also partly matches that of the experiment. So it is suggested that both of the structures are presented in the products.

$[Pb_4C_6H_5]^-$. The calculations reveal that the ground state of $[Pb_4C_6H_5]^-$ is structure **4a**, and its energy is 0.79 eV lower than the second lower energy structure **4b**. And for neutral $Pb_4C_6H_5$, the energy difference between **4a** and **4b** is only 0.17 eV. The

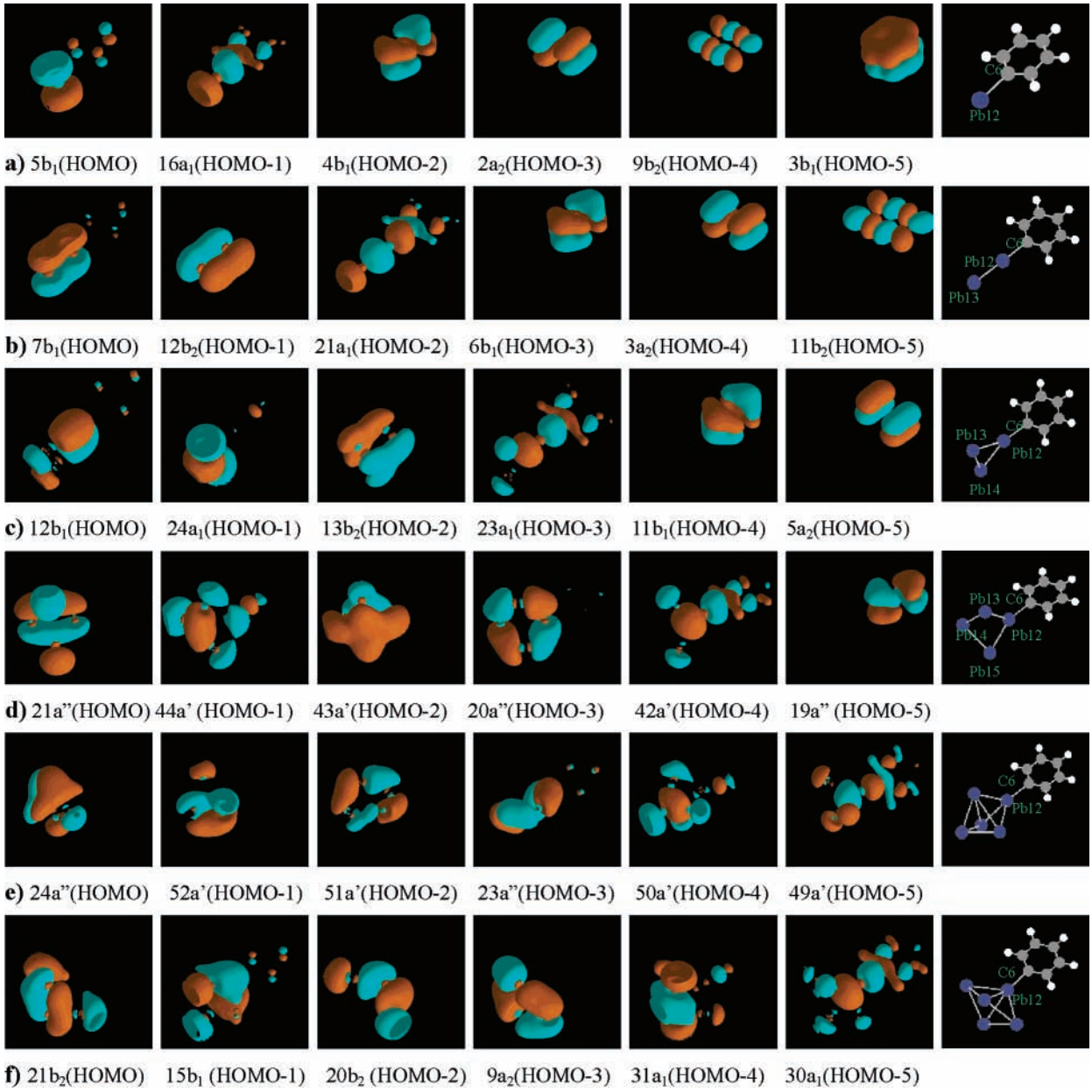

Figure 8. Molecular orbital pictures for (a) $[PbC_6H_5]^-$, (b) $[Pb_2C_6H_5]^-$, (c) $[Pb_3C_6H_5]^-$, (d) $[Pb_4C_6H_5]^-$, (e) $[Pb_5C_6H_5]^-$ (structure **5a**), and (f) $[Pb_5C_6H_5]^-$ (structure **5b**). The last picture in each row is the coordinate sketch of the cluster complex corresponding to its molecular orbital pictures.

EA of structure **4a** is 2.13 eV, to be consistent with the experimental value of 2.35 eV. As shown in Figure 6, the DOS of structure **4a** also have a good agreement with measured PES. So the **4a** can be considered as the dominant $[Pb_4C_6H_5]^-$ in the cluster distribution. The calculated EA of structure **4b** is 1.51 eV, which is much smaller than the experimental EA. This value of 1.51 eV is close to that of the lower binding energy side of the broad PES of $[Pb_4C_6H_5]^-$. So the calculated value can be evidence that the isomer (structure **4b**) exists for $[Pb_4C_6H_5]^-$ with a much lower abundance.

$[Pb_5C_6H_5]^-$. For the neutral and the anion, two low-energy structures, **5a** and **5b**, are found. The energy difference between the two structures is 0.24 eV for anions and 0.18 eV for neutrals. The EAs of structures **5a** and **5b** are 2.51 and 2.45 eV, respectively. They are in good agreement with the experimental results of 2.29 eV. The calculated and GKT-shifted DOS of structures **5a** and **5b** are shown in Figure 7. The two calculated DOS are not matched well with the PES spectra. For structure **5a**, the distribution of DOS stick spectrum is similar to that of PES, but the energy gaps of the theoretical DOS are much smaller than those of the PES. This characteristic, i.e., the calculated energy gaps are smaller than that of experimental PES, can also be seen for other clusters (Figures 3−6). But for structure **5a** the difference between the two gaps, theoretical and experimental, is larger than others. For structure **5b**, the DOS stick spectrum can match well with the two low-energy features of the PES. Therefore, neither of the two low-energy structures can be excluded by the DOS analysis. A further investigation is needed for this complex. Here we suggest that the PES of $[Pb_5C_6H_5]^-$ can be considered as contributions from both structures **5a** and **5b**.

4.4. Orbital Composition and Bonding. We have also analyzed the orbital compositions for the anion complexes, and the MO pictures from the calculated $[Pb_nC_6H_5]^-$ are given in

Figure 8. For $[PbC_6H_5]^-$ as shown in Figure 8a, the HOMO is mostly from the $6p_x$ of Pb atoms, and it is a nonbonding MO for the Pb−C part. The HOMO-1 ($16A_1$) is formed by interaction from 6s and $6p_z$ of the Pb atom with $11a_1$ of C_6H_5 (mainly formed with C6: $2p_z$, see ref 47), and it is a σ MO for the Pb−C part. Following the HOMO-1, the inner MOs of $[PbC_6H_5]^-$ are only from the C_6H_5 part, which are nonbonding MOs for the Pb−C part. Therefore, the Pb atom and the phenyl group bind together by the σ bond, in which 6s and $6p_z$ orbits of the Pb atom hybridize and then bond with the $2p_z$ orbit of the nearest C6 atom. As for $[Pb_2C_6H_5]^-$, the HOMO is from the $6p_x$ interaction of Pb12 and Pb13 atoms and the HOMO-1 is from the $6p_y$ interaction of Pb12 and Pb13 atoms. These two MOs are local π-type bonds between Pb and Pb. The HOMO-2 ($21a_1$) is formed by interaction from 6s and $6p_z$ of Pb atoms with $11a_1$ of C_6H_5 and it is a σ MO for the Pb−C part. And the inner MOs are similar with the case of $[PbC_6H_5]^-$, with nonbonding MOs for the Pb−C part. Therefore, the Pb12 atom and the phenyl group bind together by the σ bond, in which 6s and $6p_z$ orbits of the Pb atom hybridize and then bond with the $2p_z$ orbital of the nearest C6 atom.

There are two possible isomeric structures of $[Pb_3C_6H_5]^-$, so we investigate the MOs and bonding for the two isomers **3a** and **3b**. In structures **3a** and **3b** their MOs near HOMO are similar, so as an example, the MO pictures are only given for structure **3a** in Figure 8c. The HOMO, HOMO-1, and HOMO-2 are mostly the local MOs between Pb atoms (shown in Figure 8c). Only the HOMO-3 is a σ MO for the Pb−C part, and the inner MOs also are nonbonding MOs for the Pb−C part. So we conclude that in $[Pb_3C_6H_5]^-$ the Pb_3 cluster connects with the phenyl group by the Pb−C σ bond. Similar cases can be seen for the rest of the anion complexes $[Pb_mC_6H_5]^-$ ($m = 3-5$) in Figure 8d−f, and there is only one σ MO for the Pb−C part, and for all $[Pb_mC_6H_5]^-$ complexes the number of outer local MOs (meaning the MOs with the higher energy level of the assigned σ MO for the Pb−C part) between Pb atoms is equal to the number of Pb atoms. This result also indicates that the PES features for larger m of $[Pb_mC_6H_5]^-$ are like the PES of Pb_m^-. As shown in Figure 1, the PES of $[Pb_5C_6H_5]^-$ has similar characteristics as PES of Pb_5^-, which has good agreement with the predicted result of the DFT calculations.

For each of the $[Pb_mC_6H_5]^-$ complexes, there exists only one σ MO for the Pb−C part, which can be evidence that phenyl group binds on lead clusters through the Pb−C σ bond. This interaction can also influence the energy level of the outer MOs to result in the electron detachment threshold of $[Pb_mC_6H_5]^-$ complexes being higher than that of Pb_m^-. As for the exceptional $[Pb_5C_6H_5]^-$, although this also has a σ MO for the Pb−C part, the calculated EAs of **5a** and **5b** are agreement with the measured EA of $[Pb_5C_6H_5]^-$ and have a much closer value to the EA of Pb_5^-. The reason as mentioned in part 3 is that the Pb_5^- part of the $[Pb_5C_6H_5]^-$ cluster has a stable trigonal bipyramid structure similar with that of the pure Pb_5^-. Theoretic calculation also proved that Pb_5 has a trigonal bipyramid structure in both structures **5a** and **5b**, and the bonding orbit between Pb atoms and phenyl is the very inner HOMO-5 (shown in Figure 8e,f).

5. Conclusions

Phenyl−lead complexes with 1−5 lead atoms are produced from the reactions between benzene and lead vapor generated by laser ablation on a lead solid sample. EAs of Pb_m−phenyl ($m = 1-5$) and Pb_m are obtained from the photoelectron spectra with a 308 nm laser. It is found that the EAs of Pb_m−phenyl are higher than that of pure Pb_m and are similar to that of Pb_mF,[26] in which the F atom combines on lead clusters with a single chemical bond. This can be evidence that the Pb_m−phenyl anion has a closed shell electron structure and the phenyl group binds on lead clusters through the Pb−C σ bond. This conclusion has been proved by theoretic molecular orbital analysis extracted from the DFT calculation.

For each species, the theoretical EAs are in good agreement with EAs from PES. By comparison of the experimentally measured PES and DOS calculated by the relativistic DFT, we assigned the most possible structures. In summary, all the assigned structures $[Pb_mC_6H_5]^-$ ($m = 1-5$) present a closed shell electron ground-state structure, and the phenyl group binds on lead clusters through the Pb−C σ bond. For $[Pb_2C_6H_5]^-$, the actual structure of the products is not the lowest energy structure. For $[Pb_5C_6H_5]^-$, the calculated DOS of the two lower energy structures all partly match with the experimental PES, so it is suggested that the PES of $[Pb_5C_6H_5]^-$ is the contributions from the structures **5a** and **5b**.

Acknowledgment. We gratefully acknowledge the support of the National Natural Science Foundation of China under Grant Nos. 20203020 and 20433080. We thank Professor Qihe Zhu for is original design and assembly of the experimental apparatus.

References and Notes

(1) Mulliken, R. S. *J. Am. Chem. Soc.* **1952**, *64*, 811.
(2) Haaland, A. *Acta Chem. Scand.* **1965**, *19*, 41.
(3) Jacobson, D. B.; Freiser, B. S. *J. Am. Chem. Soc.* **1984**, *106*, 3900.
(4) Trevor, D. J.; Whetten, R. L.; Cox, D. M.; Kaldor, A. *J. Am. Chem. Soc.* **1985**, *107*, 518.
(5) Ma, J. C.; Dlugherty, D. A. *Chem. Rev.* **1997**, *97*, 1303.
(6) Meyer, F.; Khan, F. A.; Armentrout, P. B. *J. Am. Chem. Soc.* **1995**, *117*, 9740.
(7) Chen, Y. M.; Armentrout, P. B. *Chem. Phys. Lett.* **1993**, *210*, 123.
(8) Amicangelo, J. C.; Armentrout, P. B. *J. Phys. Chem. A* **2000**, *104*, 11420.
(9) Gerhards, M.; Thomas, O. C.; Nilles, J. M.; Zheng, W. J.; Bowen, K. H. *J. Chem. Phys.* **2002**, *116*, 10247.
(10) Zheng, W. J.; Nilles, J. M.; Thomas, O. C.; Bowen, K. H. *J. Chem. Phys.* **2005**, *122*.
(11) Zheng, W. J.; Nilles, J. M.; Thomas, O. C.; Bowen, K. H. *Chem. Phys. Lett.* **2005**, *401*, 266.
(12) Luttgens, G.; Pontius, N.; Friedrich, C.; Klingeler, R.; Bechthold, P. S.; Neeb, M.; Eberhardt, W. *J. Chem. Phys.* **2001**, *114*, 8414.
(13) Willey, K. F.; Cheng, P. Y.; Bishop, M. B.; Duncan, M. A. *J. Am. Chem. Soc.* **1991**, *113*, 4721.
(14) Willey, K. F.; Yeh, C. S.; Robbins, D. L.; Duncan, M. A. *J. Phys. Chem.* **1992**, *96*, 9106.
(15) van Heijnsbergen, D.; von Helden, G.; Meijer, G.; Maitre, P.; Duncan, M. A. *J. Am. Chem. Soc.* **2002**, *124*, 1562.
(16) Kurikawa, T.; Takeda, H.; Hiranok, M.; Judai, K.; Arita, T.; Nagao, S.; Nakajima, A.; Kaya, K. *Organometallics* **1999**, *18*, 1430.
(17) Hoshino, K.; Kurikawa, T.; Takeda, H.; Nakajima, A.; Kaya, K. *J. Phys. Chem.* **1995**, *99*, 3053.
(18) Kurikawa, T.; Hirano, M.; Takeda, H.; Yagi, K.; Hoshino, K.; Nakajima, A.; Kaya, K. *J. Phys. Chem.* **1995**, *99*, 16248.
(19) Kandalam, A. K.; Rao, B. K.; Jena, P.; Pandey, R. *J. Chem. Phys.* **2004**, *120*, 10414.
(20) Pandey, R.; Rao, B. K.; Jena, P.; Blanco, M. A. *J. Am. Chem. Soc.* **2001**, *123*, 3799.
(21) Rao, B. K.; Jena, P. *J. Chem. Phys.* **2002**, *117*, 5234.
(22) Majumdar, D.; Roszak, S.; Balasubramanian, K. *J. Chem. Phys.* **2001**, *114*, 10300.
(23) Rao, B. K.; Jena, P. *J. Chem. Phys.* **2002**, *116*, 1343.
(24) Dai, D. G.; Balasubramanian, K. *Chem. Phys. Lett.* **1997**, *271*, 118.
(25) Zhao, C. Y.; Balasubramanian, K. *J. Chem. Phys.* **2002**, *116*, 10287.
(26) Negishi, Y.; Kawamata, H.; Nakajima, A.; Kaya, K. *J. Electron Spectrosc. Relat. Phenom.* **2000**, *106*, 117.
(27) Wang, B. L.; Zhao, J. J.; Chen, X. S.; Shi, D. N.; Wang, G. H. *Phys. Rev. A* **2005**, *71*, 033201.
(28) Tang, I. N.; Castleman, A. W. *J. Chem. Phys.* **1972**, *57*, 3638.
(29) Guo, B. C.; Purnell, J. W.; Castleman, A. W. *Chem. Phys. Lett.* **1990**, *168*, 155.

(30) Xing, X. P.; Tian, Z. X.; Liu, H. T.; Tang, Z. C. *J. Phys. Chem. A* **2003**, *107*, 8484.
(31) Gantefor, G.; Gausa, M.; Meiwes-Broer, K. H.; Lutz, H. O. *Z. Phys. D* **1989**, *12*, 405.
(32) Luder, C.; Meiwes-Broer, K. H. *Chem. Phys. Lett.* **1998**, *294*, 391.
(33) Ho, J.; Polak, M.; Lineberger, W. C. *J. Chem. Phys.* **1992**, *96*, 144.
(34) Xing, X. P.; Tian, Z. X.; Liu, P.; Gao, Z.; Zhu, Q.; Tang, Z. C. *Chin. J. Chem. Phys.* **2002**, *15*, 83.
(35) Xing, X. P.; Liu, H. T.; Sun, S. T.; Cao, Y. L.; Tang, Z. C. *Chin. J. Chem. Phys.* **2004**, *17*, 321.
(36) Perdew, J. P.; Wang, Y. *Phys. Rev. B* **1992**, *45*, 13244.
(37) Lenthe, E. V.; Baerends, E. J.; Snijders, J. G. *J. Chem. Phys.* **1993**, *99*, 4597.
(38) Li, J.; Li, X.; Zhai, H. J.; Wang, L. S. *Science* **2003**, *299*, 864.
(39) Jonathan, C. R.; Gregory, S. T.; Henry, F. S.; Sreela, N.; Ellison, G. B. *Chem. Rev.* **2002**, *102*, 231.
(40) Ren, X. L.; Ervin, K. M. *Chem. Phys. Lett.* **1992**, *198*, 229.
(41) Häkkinen, H.; Moseler, M.; Kostko, O.; Morgner, N.; Hoffmann, M. A.; Issendorff, B. V. *Phys. Rev. Lett.* **2004**, *93*, 93401.
(42) Hakkinen, H.; Moseler, M.; Landman, U. *Phys. Rev. Lett.* **2002**, *89*, 33401.
(43) Hakkinen, H.; Yoon, B.; Landman, U.; Li, X.; Zhai, H. J.; Wang, L. S. *J. Phys. Chem. A* **2003**, *107*, 6168.
(44) Li, X.; Kiran, B.; Li, J.; Zhai, H. J.; Wang, L. S. *Angew. Chem., Int. Ed* **2002**, *41*, 4786.
(45) Wang, L. S.; Wang, X. B.; Wu, H.; Cheng, H. *J. Am. Chem. Soc.* **1998**, *120*, 6556.
(46) Tozer, D. J.; Handy, N. C. *J. Chem. Phys.* **1998**, *109*, 10180.
(47) Sun, S. T.; Xing, X. P.; Liu, H. T.; Tang, Z. C. *J. Phys. Chem. A* **2005**, 109, 11742.